Catalysis Today xxx (2013) xxx–xxx

Contents lists available at SciVerse ScienceDirect

Catalysis Today

journal homepage: www.elsevier.com/locate/cattod

Synthesis of lower olefins by hydrogenation of carbon dioxide over supported iron catalysts

Jingjuan Wang, Zhenya You, Qinghong Zhang, Weiping Deng, Ye Wang*

State Key Laboratory of Physical Chemistry of Solid Surfaces, National Engineering Laboratory for Green Chemical Productions of Alcohols, Ethers and Esters, College of Chemistry and Chemical Engineering, Xiamen University, Xiamen 361005, China

ARTICLE INFO

Article history:
Received 29 October 2012
Received in revised form 15 March 2013
Accepted 26 March 2013
Available online xxx

Keywords:
Carbon dioxide
Hydrogenation
Lower olefins
Fe/ZrO_2 catalyst
Alkali metal ion promoter

ABSTRACT

The hydrogenation of carbon dioxide to lower (C_2–C_4) olefins is an important reaction for the utilization of CO_2 as a carbon feedstock for the production of building-block chemicals. We found that an Fe/ZrO_2 catalyst could catalyze the hydrogenation of CO_2, but the main products were CH_4 and lower (C_2–C_4) paraffins. The modification of the Fe/ZrO_2 catalyst by alkali metal ions except for Li^+ significantly decreased the selectivities to CH_4 and lower paraffins and increased those to lower olefins and C_{5+} hydrocarbons, particularly C_{5+} olefins. The modification by Na^+, K^+, or Cs^+ also increased the conversion of CO_2. The best performance for lower olefin synthesis was obtained over the K^+-modified Fe/ZrO_2 catalyst with a proper K^+ content (0.5–1.0 wt%). Among several typical supports including SiO_2, Al_2O_3, TiO_2, ZrO_2, mesoporous carbon, and carbon nanotube, ZrO_2 provided the highest selectivity and yield to lower olefins. Our characterizations suggest that the modification by K^+ accelerates the generation of χ-Fe_5C_2 phase under the reaction conditions. This together with the decreased hydrogenation ability in the presence of K^+ has been proposed to be responsible for the enhanced selectivity to lower olefins.

1. Introduction

The concerns on the emissions of CO_2, which is a major anthropogenic greenhouse gas, have grown rapidly in recent years because of the worsening global environment. This has driven research activities in the capture and transformation of CO_2 [1–5]. The diminishing of fossil resources has also increased the research interests in the utilization of CO_2 as an alternative carbon feedstock for the production of chemicals and fuels [6–10]. CO_2 possesses advantages of being nontoxic, abundant, and renewable as a chemical feedstock. However, the conversion of CO_2 typically requires external energy input such as photo or electric energy [11–13] and/or high energy co-reactants such as H_2 and reactive organic compounds (e.g., epoxide) [7] because CO_2 is a highly stable molecule. Although there are only limited industrial processes utilizing CO_2 at this moment, many promising reactions for the transformation of CO_2 have been reported [6–10].

Among various transformations of CO_2, the hydrogenation of CO_2 is a versatile route capable of producing various chemicals such as methanol, higher alcohols, formic acid, CH_4, and C_{2+} hydrocarbons [10,14]. Lower (C_2–C_4) olefins are important building-block chemicals and are currently being produced mainly from petroleum by steam-cracking of naphtha. Numerous studies have been contributed to producing lower olefins through non-petroleum routes such as the dehydrogenation of lower paraffins [15], the two-step process from methane [16,17], and the conversion of synthesis gas, which may be obtained from natural gas, coal or biomass, either directly [18] or via methanol [19]. The production of lower olefins by the hydrogenation of CO_2, which is an exothermic reaction (Eq. (1)), would be highly desirable from the viewpoint of utilizing CO_2 as a carbon feedstock for the production of building-block chemicals.

$$nCO_2 + 3nH_2 \rightarrow C_nH_{2n} + 2nH_2O \quad \Delta_r H_{573\ K} = -128\ \text{kJ mol}^{-1} \quad (1)$$

Iron-based catalysts have been studied for the hydrogenation of CO_2 to C_{2+} hydrocarbons [20–31], but only a few of these studies have focused on the formation of lower olefins [24,25,31]. It is generally accepted that, instead of direct hydrogenation of CO_2, the reverse water-gas shift reaction (Eq. (2)) proceeds over these catalysts, followed by the hydrogenation of CO to hydrocarbons (Eq. (3)) via the Fischer–Tropsch (FT) mechanism. Fe-based catalysts can catalyze both the reverse water–gas shift reaction [32,33] and the hydrogenation of CO to light olefins [18], and thus, are expected to show good performances for the hydrogenation of CO_2 to C_2–C_4 olefins.

$$CO + H_2 \rightarrow CO + H_2O \quad \Delta_r H_{573\ K} = 38\ \text{kJ mol}^{-1} \quad (2)$$

$$nCO + 2nH_2 \rightarrow C_nH_{2n} + nH_2O \quad \Delta_r H_{573\ K} = -166\ \text{kJ mol}^{-1} \quad (3)$$

* Corresponding author. Tel.: +86 592 2186156; fax: +86 592 2183047.
E-mail address: wangye@xmu.edu.cn (Y. Wang).

0920-5861/$ – see front matter © 2013 Elsevier B.V. All rights reserved.
http://dx.doi.org/10.1016/j.cattod.2013.03.031

However, the selectivity to C_2–C_4 olefins is still low in the hydrogenation of CO_2 over most of the reported catalysts. It can be expected that both the support and the promoter may affect the activity and the selectivity of Fe-based catalysts. However, little information is available on how to increase the selectivity to lower olefins. Undoubtedly, more fundamental studies are needed to develop an efficient Fe-based catalyst for the selective production of C_2–C_4 olefins from CO_2. This paper reports our recent studies on the effects of alkali metal ions on the hydrogenation of CO_2 to C_2–C_4 olefins over supported Fe catalysts.

2. Experimental

2.1. Catalyst preparation

Metal oxide supports including SiO_2, TiO_2, Al_2O_3, and ZrO_2 were purchased from Alfa Aesar (for ZrO_2) or Sinopharm Chemical Reagent Co. (for the other metal oxides). Carbon nanotubes (CNTs) were synthesized by a method reported previously [34], and were pretreated with a 68 wt% nitric acid at 393 K to remove the Ni catalyst used for CNT synthesis, followed by washing and drying. The supported Fe catalysts were prepared by the conventional impregnation method. For example, for the preparation of the 10 wt% Fe/ZrO_2 catalyst, ZrO_2 (4.5 g) was first added into an aqueous solution of $Fe(NO_3)_3$ (0.2 mol dm^{-3}, 45 mL). The suspension was then stirred for 8 h, followed by evaporation at 353 K to dryness. The obtained powdery catalyst was further dried at 393 K for 12 h and calcined in air at 773 K for 5 h. The alkali metal ion-modified supported Fe catalysts were prepared by a co-impregnation method using a mixed aqueous solution containing certain amount of an alkali metal salt ($LiNO_3$, $NaNO_3$, KNO_3, RbCl or CsCl) and $Fe(NO_3)_3$ with a similar procedure.

2.2. Catalyst characterization

X-ray diffraction (XRD) measurements were carried out on a Panalytical X'pert Pro Super X-ray diffractometer with Cu-K_α radiation (40 kV and 30 mA). For in situ XRD measurements, the powdery sample was loaded into an XRK-900 cell, which was directly attached with the X-ray diffractometer. The XRD pattern for the fresh sample was first recorded. Then, a H_2 gas flow with a flow rate of 50 mL min^{-1} was introduced into the XRK-900 cell and the temperature was raised at a rate of 10 K min^{-1}. When the desired temperature was reached, the catalyst was kept at that temperature for 5 min, and the XRD pattern was recorded. 25 min were typically required for the collection of one pattern with 2θ ranging from 20° to 50°. Before the appearance of the characteristic peaks ascribed to Fe species (32°–45°), the catalyst had been kept at the desired temperature for >15 min. The in situ XRD patterns under the reactant gas mixture of ($H_2 + CO_2$) were also recorded at 618 K. For these measurements, the sample was first reduced in the in situ XRK-900 cell with H_2 gas flow with a rate of 50 mL min^{-1} at 673 K. After being cooled down to 618 K, the reactant gas mixture was introduced to the in situ XRK-900 cell, and then the XRD pattern was recorded after a certain time.

CO_2 temperature-programmed desorption (CO_2-TPD) was performed on a Micromeritics AutoChem 2920II instrument. Typically, the sample loaded in a quartz reactor was first pretreated with high-purity He at 623 K for 1 h. After the sample was cooled down to 373 K, CO_2 adsorption was performed by switching the He flow to a CO_2–He (10 vol% CO_2) gas flow and then keeping at 373 K for 1 h. Then, the gas phase or the weakly adsorbed CO_2 was purged by high-purity He at the same temperature. CO_2-TPD was performed in the He flow by raising the temperature to 1073 K at a rate of 10 K min^{-1}, and the desorbed CO_2 molecules were detected by ThermoStar GSD 301 T2 mass spectrometer with the signal of $m/e = 44$.

2.3. Catalytic reaction

Catalytic reactions were performed on a high-pressure fixed-bed flow reactor. The catalyst (typically 1.0 g) loaded in the reactor was first reduced by H_2 with a flow rate of 50 mL min^{-1} at 673 K for 5 h. After the catalyst was cooled down to 353 K, a reactant gas mixture of ($H_2 + CO_2$) with a H_2/CO_2 molar ratio of 3.0 and a flow rate of 20 mL min^{-1}, which contained 5% argon as an internal standard for the calculation of CO_2 conversions, was introduced to the reactor. Then, the pressure and temperature were increased typically to 2.0 MPa and 613 K, respectively. The products were analyzed by online gas chromatography. The data at steady states, which were obtained typically after 10 h of reaction, were used for discussion.

3. Results and discussion

3.1. Catalytic behaviors of Fe-based catalysts for hydrogenation of CO_2

3.1.1. Effect of modification by alkali metal ions on catalytic behaviors of Fe/ZrO_2 catalysts

It has been demonstrated that ZrO_2 is a unique support for the hydrogenation of CO_2 to CH_3OH or CH_4 when Cu, Ag or Ni is used as the active metal [35]. However, few studies have used ZrO_2 for the hydrogenation of CO_2 to hydrocarbons. Here, we first investigated the catalytic behavior of the Fe/ZrO_2 catalyst for the hydrogenation of CO_2. The conversion of CO_2 was 32% over the 10 wt% Fe/ZrO_2 under our reaction conditions (Table 1). The selectivity to CO was 25% and that to hydrocarbons (C_nH_m) was 75% over this catalyst. CH_4 and C_2–C_4 paraffins were the dominant products in hydrocarbons. Thus, the Fe/ZrO_2 catalyst without modification is not suitable for the hydrogenation of CO_2 to lower olefins.

We investigated the effect of the modification by alkali metal ions on catalytic behaviors of the Fe/ZrO_2 catalyst. Table 1 shows that the addition of Li^+ decreases the conversion of CO_2. The selectivity to hydrocarbons also became lower while that to CO became higher by the addition of Li^+ to the Fe/ZrO_2 catalyst. These indicate that Li^+ suppresses both the reverse water-gas shift reaction and the hydrogenation of CO to hydrocarbons. The inhibiting roles of Li^+ in the water-gas shift and FT reactions were reported in previous studies [36,37]. The distribution of hydrocarbons did not change significantly after the modification by Li^+; CH_4 and C_2–C_4 paraffins were still the dominant products. This indicates that the presence of Li^+ in the Fe/ZrO_2 does not affect the ability of catalyst for the hydrogenation of CH_x intermediates or olefins, which are believed to be the primary products, but decreases the ability of catalyst for the activation of CO and CO_2. On the other hand, the addition of other alkali metal ions to the Fe/ZrO_2 catalyst did not decrease the conversion of CO_2. The modification by Na^+, K^+ and Cs^+ rather increased the conversion of CO_2. Particularly, K^+ showed a significant enhancing effect on the catalytic activity, while the promoting effects of Rb^+ and Cs^+ were less significant on CO_2 conversions. This might be caused by the residual chlorine [38], since RbCl and CsCl were used as the precursors. The selectivity to CO decreased from 25% to 15–21% after the modification by Na^+, K^+, Rb^+, or Cs^+. Organic oxygenates were also formed with considerable selectivities (17–20%) in addition to hydrocarbons over these catalysts. More significantly, the modification of the Fe/ZrO_2 catalyst by Na^+, K^+, Rb^+ or Cs^+ remarkably changed the hydrocarbon distributions. The fractions of CH_4 and C_2–C_4 paraffins decreased significantly from 70% to 18–26% and from 29% to <10%, respectively. Simultaneously, the fractions of C_2–C_4 olefins and C_{5+} hydrocarbons increased

Please cite this article in press as: J. Wang, et al., Synthesis of lower olefins by hydrogenation of carbon dioxide over supported iron catalysts, Catal. Today (2013), http://dx.doi.org/10.1016/j.cattod.2013.03.031

Table 1
Catalytic performances of alkali metal ion-modified 10 wt% Fe/ZrO_2 catalysts for the hydrogenation of CO_2[a]

Alkali metal[b]	CO_2 conv. (%)	Select.[c] (%)		Hydrocarbon distribution[d] (%)					$C_{2-4}^{=}$ yield (%)
		CO	C_nH_m	CH_4	$C_{2-4}^{=}$	C_{2-4}^{0}	$C_{5+}^{=}$	C_{5+}^{0}	
Non	32	25	75	70	0.1	29	0.4	0.5	0
Li^+	26	42	56	68	1.4	30	0.1	0.5	0.20
Na^+	39	21	59	21	49	8.8	15	6.2	11
K^+	43	15	66	18	44	9.2	19	9.8	13
Rb^+	31	15	68	19	43	8.0	19	11	9.1
Cs^+	39	16	67	26	43	9.6	14	7.4	11

[a] Reaction conditions: W (catalyst) = 1.0 g, $H_2/CO_2 = 3$, $T = 613$ K, $P = 2$ MPa, $F = 20$ mL min^{-1}, time on stream = 10 h.
[b] The content of alkali metal ion was 1.0 wt%.
[c] C_nH_m denotes hydrocarbons, and the other products were organic oxygenates.
[d] $C_{2-4}^{=}$: C_2–C_4 olefins; C_{2-4}^{0}: C_2–C_4 paraffins; $C_{5+}^{=}$: C_{5+} olefins; C_{5+}^{0}: C_{5+} paraffins.

dramatically from 0.1% to >40% and from 0.5% to >20%, respectively. The ratios of olefins to paraffins in C_2–C_4 hydrocarbons over these modified catalysts were >4.4. Olefins also dominated the C_{5+} hydrocarbons, and the ratio of olefins to paraffins in C_{5+} hydrocarbons was around 2 over the Na^+, K^+, Rb^+ or Cs^+-modified Fe/ZrO_2 catalyst. These observations allow us to consider that the modification by alkali metal ions except for Li^+ can decrease the hydrogenation ability and increase the chain-growth probability. Among these alkali metal ion-modified catalysts, the K^+-Fe/ZrO_2 exhibited the highest yield to C_2–C_4 olefins (13%).

3.1.2. Effect of support on catalytic behaviors of K^+-modified Fe catalysts

We investigated the effect of support on catalytic performances of the K^+-modified Fe catalysts. Table 2 shows that support can affect not only the activity but also the product selectivity. The use of SiO_2 as a support showed both a lower conversion of CO_2 and a lower selectivity to hydrocarbons, and thus was unsuitable for the hydrogenation of CO_2 to hydrocarbons. Iron catalysts loaded on other typical metal oxide supports such as Al_2O_3, TiO_2, and ZrO_2 in the presence of K^+ provided much better performances for the hydrogenation of CO_2 to lower olefins. Among these metal oxides, ZrO_2 was the most active and selective support for the conversion of CO_2 to C_2–C_4 olefins. A carbon nanofiber (CNF)-supported Fe catalyst was recently demonstrated to exhibit excellent catalytic performances for the hydrogenation of CO to lower olefins [18]. We examined the catalytic performances of modified Fe catalysts loaded on two carbon materials, i.e., mesoporous carbon (meso-C) and CNT. The K^+-Fe/CNT catalyst showed a better performance for the hydrogenation of CO_2 to lower olefins, affording a C_2–C_4 olefin yield of 8.8%. The conversion of CO_2 and the selectivity to lower olefins over the K^+-Fe/CNT catalyst were, however, both lower than those over the K^+-Fe/ZrO_2 catalyst.

3.1.3. Effect of K^+ content on catalytic behaviors of K^+-modified Fe/ZrO_2 catalysts

Although an appropriate support is important for obtaining higher activity and higher C_2–C_4 olefin selectivity, the presence of an alkali metal ion plays an essential role in the hydrogenation of CO_2 to C_2–C_4 olefins. To gain further insights into the function of K^+, we investigated the effect of K^+ content on catalytic performances of the K^+-Fe/ZrO_2 catalysts. Fig. 1A shows that the modification by K^+ with a proper content (0.1–5.0 wt%) can increase the conversion of CO_2. When the K^+ content exceeded 5.0 wt%, the conversion of CO_2 decreased again. The selectivities to CO and hydrocarbons both decreased slightly with increasing K^+ content to 0.5 wt% (Fig. 1B). At the same time, the selectivity to oxygenates increased from 0.4% to ~20%. Inside the hydrocarbons, the fractions of CH_4 and C_2–C_4 paraffins decreased steeply from 70% and 29% to ~20% and ~10%, respectively, with an increase in the K^+ content to 0.5 wt% (Fig. 1C and D). At the same time, the fractions of C_{5+} hydrocarbons, particularly C_{5+} olefins, and C_2–C_4 olefins increased significantly from almost 0 to ~30% and ~45%, respectively (Fig. 1C and D). Further increases in the K^+ content did not change the fractions of CH_4, C_2–C_4 paraffins, C_2–C_4 olefins, and C_{5+} hydrocarbons. In a range of K^+ content of 0.5–5.0 wt%, the yields of C_2–C_4 olefins kept at 12–13%. A further increase in the K^+ content decreased the yield of C_2–C_4 olefins because of the decreased conversion of CO_2.

3.2. Characterizations of Fe/ZrO_2 catalysts with and without K^+ modification

To gain insights into the evolution of iron phases during the reductive pretreatment, we carried out XRD measurements for the 10 wt% Fe/ZrO_2 catalysts with and without K^+ modification in H_2 gas flow at different temperatures. The catalyst was loaded in the in situ XRD cell (XRK-900), and the XRD pattern of the fresh catalyst was first recorded. The fresh catalysts with and without K^+

Table 2
Catalytic performances of K^+ (1 wt%)-modified Fe (10 wt%) catalysts loaded on various supports for the hydrogenation of CO_2[a]

Support[b]	CO_2 conv. (%)	Select.[c] (%)		Hydrocarbon distribution[d] (%)					$C_{2-4}^{=}$ yield (%)
		CO	C_nH_m	CH_4	$C_{2-4}^{=}$	C_{2-4}^{0}	$C_{5+}^{=}$	C_{5+}^{0}	
SiO_2	7.1	92	8.1	72	18	8.6	0.1	1.3	0.10
Al_2O_3	33	17	76	17	36	6.0	28	13	9.0
TiO_2	21	55	38	22	43	7.2	18	9.8	3.4
ZrO_2	42	15	64	20	46	8.2	18	8.8	12
Meso-C	33	31	58	32	30	26	2.0	10	5.7
CNT	35	12	74	26	34	10	19	11	8.8

[a] Reaction conditions: W(catalyst) = 1.0 g, $H_2/CO_2 = 3$, $T = 613$ K, $P = 2$ MPa, $F = 20$ mL min^{-1}, time on stream = 10 h.
[b] Meso-C denotes mesoporous carbon.
[c] C_nH_m denotes hydrocarbons; the other products were CO and oxygenates.
[d] $C_{2-4}^{=}$: C_2–C_4 olefins; C_{2-4}^{0}: C_2–C_4 paraffins; $C_{5+}^{=}$: C_5^+ olefins; C_{5+}^{0}: C_{5+} paraffins.

Please cite this article in press as: J. Wang, et al., Synthesis of lower olefins by hydrogenation of carbon dioxide over supported iron catalysts, Catal. Today (2013), http://dx.doi.org/10.1016/j.cattod.2013.03.031

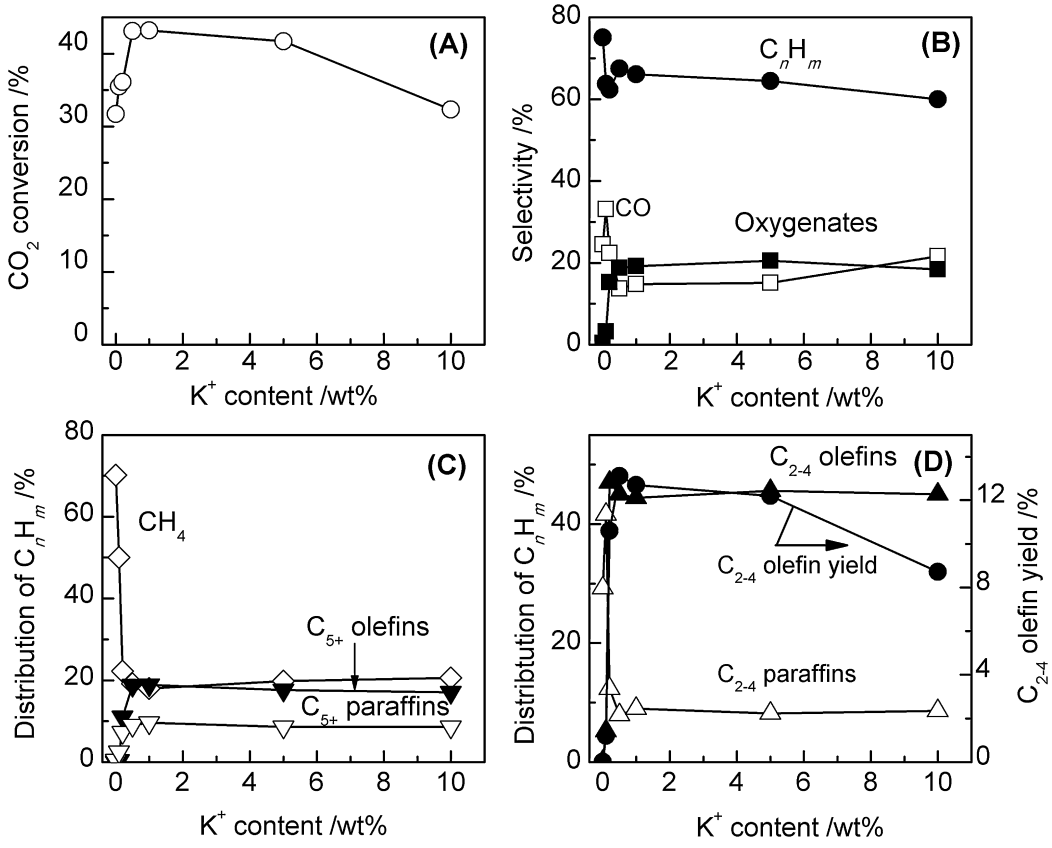

Fig. 1. Effect of K^+ content on catalytic performances of the K^+-10 wt% Fe/ZrO_2 catalysts for hydrogenation of CO_2. (A) CO_2 conversion, (B) selectivity, (C) and (D) distribution of hydrocarbons. Reaction conditions: W(catalyst) = 1.0 g, H_2/CO_2 = 3, T = 613 K, P = 2 MPa, F = 20 mL min^{-1}, time on stream = 10 h.

modification contained Fe_2O_3 as the sole iron phase besides monoclinic ZrO_2. Then, the H_2 gas with a flow rate of 50 mL min^{-1} was introduced into the cell, and the temperature was raised at a rate of 10 K min^{-1}. When the desired temperature was reached, the catalyst was kept at that temperature for 5 min, and the XRD pattern was recorded. For the Fe/ZrO_2 catalyst without K^+ modification, no significant changes were observed at temperatures ≤573 K (Fig. 2). At 673 K, the diffraction peak at 2θ of 33.2° ascribed to Fe_2O_3 disappeared, and new diffraction peaks at 2θ of 30.1°, 37.0°, and 43.0° attributed to Fe_3O_4 were observed, revealing the transformation of Fe_2O_3 to Fe_3O_4 at 673 K. Moreover, the peak at 2θ of 44.9° shifted to 44.6° and the intensity of this peak increased significantly. A further increase in the temperature to 723 K led to the disappearance of the peaks belonging to Fe_3O_4, and the further increase in the intensity of the peak at 2θ of 44.5°. It should be noted that the peak at 2θ of 44.5°–44.9° may arise from both monoclinic ZrO_2 (2θ = 44.9°) and metallic Fe (2θ = 44.5°). Because the positions and the intensities of diffraction peaks belonging to ZrO_2 alone did not change significantly with temperatures, the shift of the peak position slightly to lower diffraction angles and the significant increase in the peak intensity at higher temperatures (≥673 K) indicate the formation of metallic Fe. For the K^+-Fe/ZrO_2 catalyst under H_2 flow at different temperatures, similar XRD patterns were observed (Fig. 3). Fe_2O_3 in the fresh catalyst was completely reduced to Fe_3O_4 at 673 K under H_2 flow. The formation of metallic Fe became more significant even at 673 K from the significantly enhanced intensity of the diffraction peak at 2θ of 44.5°.

We performed in situ XRD measurements for the Fe/ZrO_2 and the K^+-Fe/ZrO_2 catalysts under gas mixture of ($H_2 + CO_2$) with a H_2/CO_2 ratio of 3. In these experiments, after reduction with H_2 at 673 K, the temperature was cooled down to 618 K, and then the reactant gas mixture was introduced to the in situ XRD cell. Fig. 4 shows that Fe_3O_4 was the main iron phase for the 10 wt% Fe/ZrO_2 catalyst under these conditions. The XRD pattern did not undergo significant changes with time on stream up to 5 h. On the other hand, for the catalyst with K^+ modification, besides the diffraction peaks at 2θ of 30.1°, 37.0°, and 43.0° belonging to Fe_3O_4, new peaks at 2θ of 43.5° and 44.2° were observed after 2 h under the ($H_2 + CO_2$) gas mixture at 618 K (Fig. 5). These two peaks could be attributed to

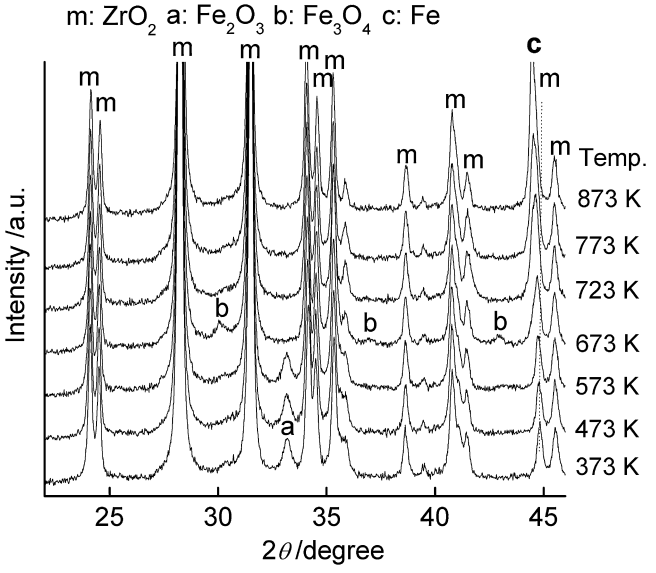

Fig. 2. In situ XRD patterns for the Fe/ZrO_2 catalyst under H_2 gas flow at different temperatures.

Please cite this article in press as: J. Wang, et al., Synthesis of lower olefins by hydrogenation of carbon dioxide over supported iron catalysts, Catal. Today (2013), http://dx.doi.org/10.1016/j.cattod.2013.03.031

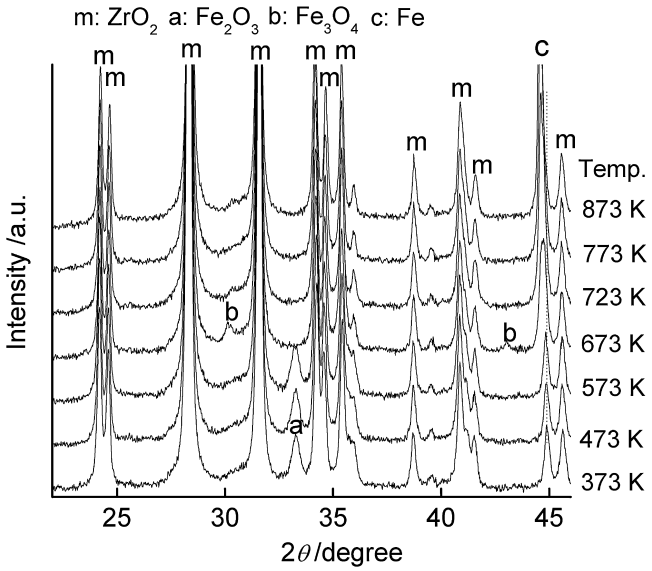

Fig. 3. In situ XRD patterns for the K^+–Fe/ZrO_2 catalyst under H_2 gas flow at different temperatures.

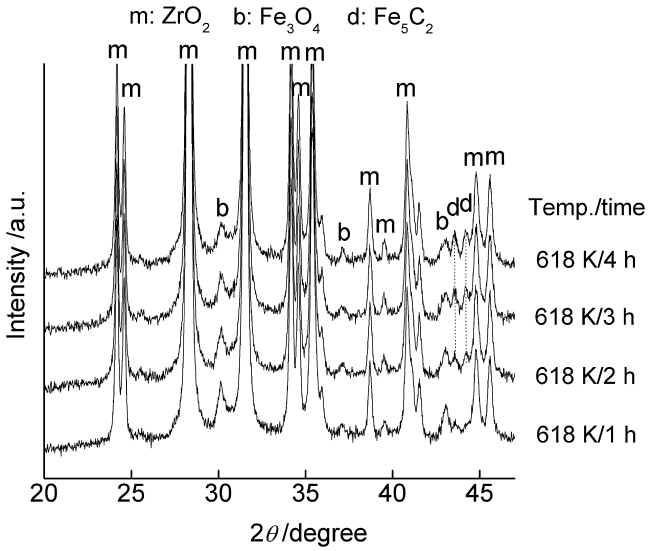

Fig. 5. In situ XRD patterns for the K^+–Fe/ZrO_2 catalyst under ($H_2 + CO_2$) ($H_2/CO_2 = 3$) gas flow at 618 K for different times.

χ-Fe_5C_2 phase. This suggests the formation of χ-Fe_5C_2 species over the K^+-modified Fe/ZrO_2 catalyst under the ($H_2 + CO_2$) gas mixture.

It should be noted that the above in situ XRD measurements were carried out under atmospheric pressure. We also measured the XRD patterns for the catalysts after reactions under 2 MPa of ($H_2 + CO_2$) at 613 K for 10 h. The results for the Fe/ZrO_2 catalysts modified by different alkali metal ions are displayed in Fig. 6. For the Fe/ZrO_2 and the Li^+–Fe/ZrO_2, the diffraction peaks at 2θ of 43.5° and 44.2° attributable to χ-Fe_5C_2 were quite weak. These two peaks became significantly stronger for the Fe/ZrO_2 catalysts containing Na^+, K^+, Rb^+, and Cs^+ modifiers. This allows us to propose that the alkali metal ions of Na^+, K^+, Rb^+, and Cs^+ are more effective for the generation of χ-Fe_5C_2 species under the reaction conditions. We further investigated the effect of K^+ content on the formation of iron carbides. Fig. 7 shows the XRD patterns after 10 h of reaction under 2 MPa ($H_2 + CO_2$) at 613 K for the K^+-10 wt% Fe/ZrO_2 catalysts with different K^+ contents. The intensities of the peaks ascribed to χ-Fe_5C_2 increased with the content of K^+ up to 0.5 wt%. This further demonstrates that K^+ accelerates the generation of χ-Fe_5C_2 under our reaction conditions.

We performed CO_2-TPD studies to gain information about the adsorption of CO_2 on the Fe/ZrO_2 catalysts with and without K^+ modification. The 10 wt% Fe/ZrO_2 catalyst without K^+ modification exhibited very weak CO_2 desorption peaks in the CO_2-TPD profile (Fig. 8). The addition of K^+ to the Fe/ZrO_2 caused the appearance of two CO_2 desorption peaks at lower (~450 K) and higher (900–965 K) temperatures. The intensities of the desorbed CO_2, particularly the one at higher temperatures, increased with the content of K^+. This observation indicates that the presence of K^+ promotes the adsorption of CO_2 onto the catalyst surface. We have quantified the amounts of CO_2 desorbed at the lower (peak at ~450 K) and the higher (peak at 900–965 K) temperatures. As displayed in Table 3, the amount of CO_2 desorbed at lower temperatures was

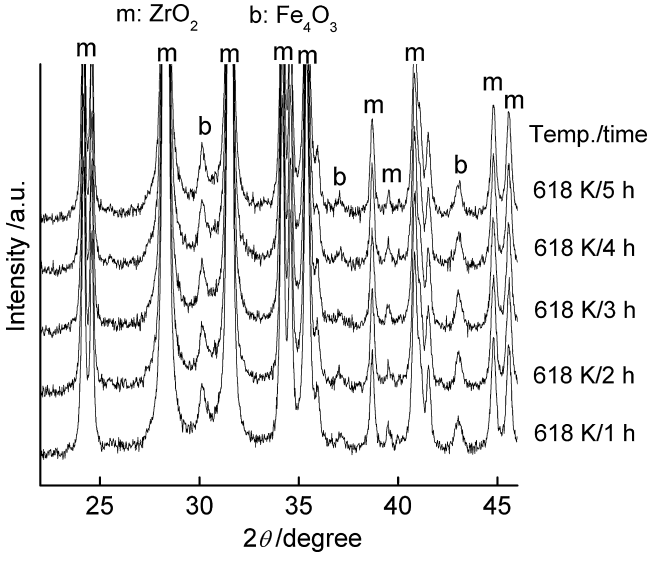

Fig. 4. In situ XRD patterns for the Fe/ZrO_2 catalyst under ($H_2 + CO_2$) ($H_2/CO_2 = 3$) gas flow at 618 K for different times.

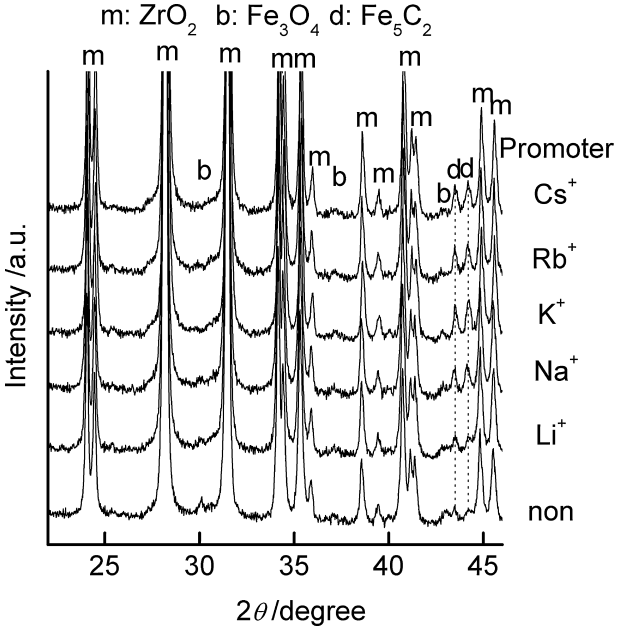

Fig. 6. XRD patterns for the Fe/ZrO_2 catalysts with different alkali metal ions after reactions. The reaction conditions were the same as those in Fig. 1.

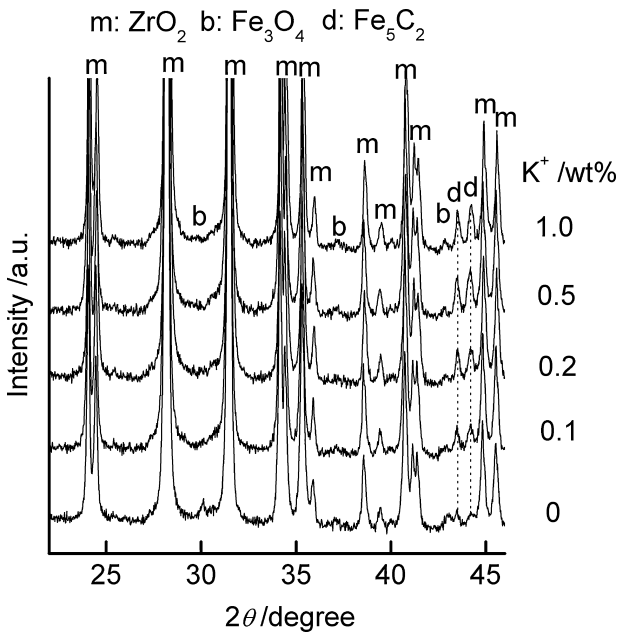

Fig. 7. XRD patterns for the K^+–Fe/ZrO_2 catalysts with different K^+ contents after reactions. The reaction conditions were the same as those in Fig. 1.

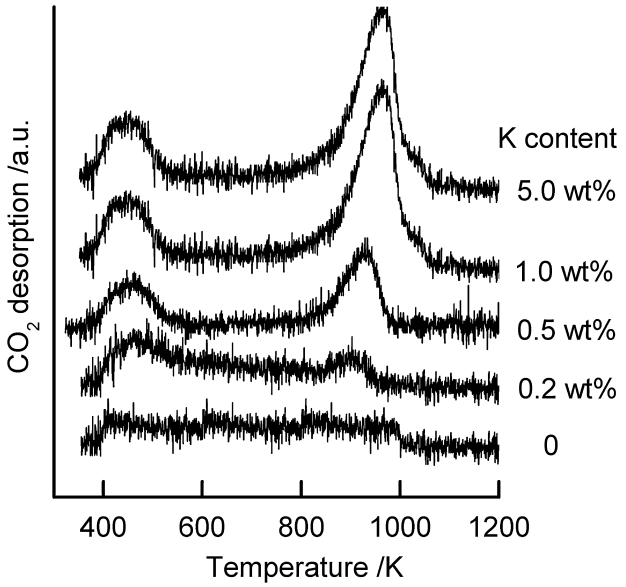

Fig. 8. CO_2-TPD profiles for the K^+–Fe/ZrO_2 catalysts with different K^+ contents.

about 2.6 times higher than that at higher temperatures for the catalyst with a K^+ content of 0.2 wt%. The increase in the K^+ content caused the increases in the amounts of CO_2 desorbed, particularly that at higher temperatures.

Table 3
Amounts of CO_2 desorption evaluated from CO_2-TPD results.

Catalyst	Amounts of CO_2 desorption (mmol g^{-1})	
	400–500 K	900–960 K
10 wt% Fe/ZrO_2	0	0
0.2 wt% K^+–10 wt% Fe/ZrO_2	20	7.6
0.5 wt% K^+–10 wt% Fe/ZrO_2	24	21
1.0 wt% K^+–10 wt% Fe/ZrO_2	30	84
5.0 wt% K^+–10 wt% Fe/ZrO_2	32	83

3.3. The roles of alkali metal ions and supports and the nature of the active Fe species

Our catalytic studies demonstrated that Fe/ZrO_2 could catalyze the hydrogenation of CO_2, but the main products were CH_4 and C_2–C_4 paraffins. The modification by alkali metal ions except for Li^+ significantly changed the product distributions; the formations of CH_4 and C_2–C_4 paraffins were dramatically suppressed, and C_2–C_4 olefins and C_{5+} hydrocarbons became the main products. The ratios of olefins to paraffins in C_2–C_4 and C_{5+} hydrocarbons were >4.4 and ~2.0 over theses alkali metal ion-modified Fe/ZrO_2 catalyst. The highest yield of C_2–C_4 olefins (13%) was obtained over the K^+-10 wt% Fe/ZrO_2 catalysts with K^+ contents of 0.5–1.0 wt%. The modification by K^+ with proper contents also enhanced CO_2 conversion.

These catalytic results have provided us information about the roles of K^+. The increase in CO_2 conversion after the addition of K^+ to the Fe/ZrO_2 catalyst suggests that K^+ may promote the activation of CO_2. It is generally accepted that the hydrogenation of CO_2 to hydrocarbons over Fe-based catalysts proceeds via a two-step mechanism or indirect mechanism, i.e., the conversion of CO_2 to CO via the reverse water–gas shift reaction and the subsequent hydrogenation of CO [20,29]. Thus, the decrease in the selectivity to CO and the increase in that to oxygenates in the presence of K^+ (Table 1 and Fig. 1) may indicate that K^+ enhances the chemisorption and the subsequent conversion of CO. However, we cannot completely exclude the possibility that the direct hydrogenation of CO_2 might also contribute to the formation of hydrocarbons, and this direct mechanism may involve the dissociation of CO_2 to carbon species, followed by hydrogenation of the adsorbed species [39]. In this case, K^+ might enhance the direct activation of CO_2 to adsorbed carbon species.

Our CO_2-TPD studies have demonstrated that the introduction of basic K^+ enhanced the adsorption of acidic CO_2 molecules (Fig. 8). This may contribute to increasing the conversion of CO_2 over the K^+-modified Fe/ZrO_2 catalysts. It is reasonable that the strongly chemisorbed CO_2 or carbonate species with a desorption peak at 900–965 K may be difficult to be hydrogenated under our reaction conditions and may not contribute to the catalytic conversion of CO_2. Thus, it is probable that the chemisorbed CO_2 species, which show a desorption peak at a lower temperature (~450 K), mainly account for the catalytic reaction. At higher K^+ contents, the formation of larger amounts of strongly chemisorbed CO_2 or carbonates on catalyst surfaces (Fig. 8 and Table 3) may lead to the lower catalytic activity (Fig. 1) because of the possible covering of the active Fe species.

Concerning the product selectivity, the decrease in the fraction of C_2–C_4 paraffins and the increases in that of C_2–C_4 olefins clearly suggest the decrease in the hydrogenation ability of the catalyst after the modification by K^+. The dramatic decrease in the fraction of CH_4 and the increase in that to C_{5+} hydrocarbons suggest the increase in the chain-growth probability over the K^+-modified catalysts. The relatively higher fraction of olefins in C_{5+} hydrocarbons also indicates that the presence of K^+ decreases the hydrogenation ability or inhibits the re-adsorption of olefins.

Our characterizations showed that the alkali metal ion promoted the generation of χ-Fe_5C_2 under the ($H_2 + CO_2$) gas mixture. The generation of χ-Fe_5C_2 was confirmed during both the in situ XRD measurements under the ($H_2 + CO_2$) gas flow (atmospheric pressure) and the XRD measurements after reactions for the catalysts with K^+ modification. Our studies suggest that there is a good correlation between the generation of χ-Fe_5C_2 and the catalytic performance for the production of C_2–C_4 olefins. Many recent studies have provided evidence that iron carbide species, particularly χ-Fe_5C_2, is an active phase for the production of C_2–C_4 olefins or C_{5+} hydrocarbons in the hydrogenation of CO, i.e., Fischer–Tropsch

Please cite this article in press as: J. Wang, et al., Synthesis of lower olefins by hydrogenation of carbon dioxide over supported iron catalysts, Catal. Today (2013), http://dx.doi.org/10.1016/j.cattod.2013.03.031

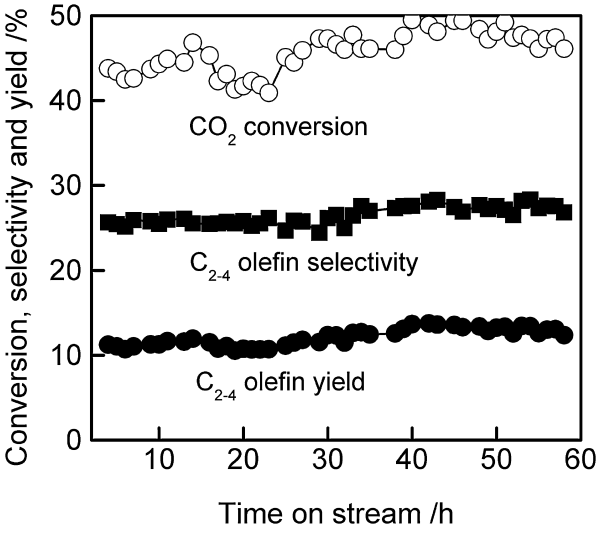

Fig. 9. Changes of catalytic performances of K^+–Fe/ZrO_2 catalyst for the hydrogenation of CO_2. Reaction conditions: W(catalyst) = 1.0 g, H_2/CO_2 = 3, T = 613 K, P = 2 MPa, F = 20 mL min^{-1}.

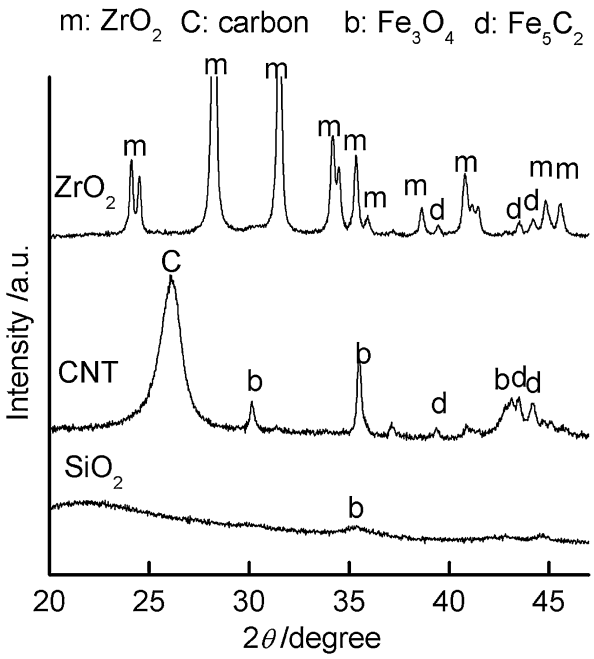

Fig. 10. XRD patterns for the K^+–Fe/ZrO_2, K^+–Fe/SiO_2, and K^+–Fe/CNT catalysts after reactions. The reaction conditions were the same as those in Fig. 1.

synthesis [32,33,40–46]. For example, Pan and co-workers once demonstrated that a higher fraction of iron carbide phase resulted in a higher C_{5+} selectivity and a lower CH_4 selectivity for the Fe catalyst confined inside the CNTs [41]. Sun et al. found that the increase in the concentration of χ-Fe_5C_2 in a Raney Fe@HZSM-5 catalyst led to a higher C_{5+} selectivity [44]. Very recently, Yang et al. reported a successful controlled synthesis of χ-Fe_5C_2 nanoparticles and found that the χ-Fe_5C_2 nanoparticles exhibited excellent catalytic performances in Fischer–Tropsch synthesis, providing higher selectivities to C_{5+} hydrocarbons and C_2–C_4 olefins as compared to the conventional H_2-reduced hematite catalyst [45]. As mentioned above, the hydrogenation of CO_2 over our catalysts mainly proceeds via the indirect mechanism, i.e., the reverse water-gas shift of CO_2 with H_2 to CO and H_2O, and the subsequent hydrogenation of CO to hydrocarbons, i.e., Fischer–Tropsch synthesis, although we cannot completely exclude the possibility of the direct hydrogenation of CO_2. Actually, the reaction conditions adopted in the present work were similar to those employed in the hydrogenation of CO to lower olefins over Fe-based catalysts except for the ratio of H_2 to CO_2 or CO [18]. Detailed analyses of the catalytic results for the hydrogenation of CO [18] and CO_2 (this work) showed similar product distributions in hydrocarbons for the two reactions. Therefore, the enhanced generation of χ-Fe_5C_2, which is an active phase for the hydrogenation of CO to C_{5+} hydrocarbons and C_2–C_4 olefins, would promote the formation of C_2–C_4 olefins in the hydrogenation of CO_2.

Based on the results and discussion described above, we propose that the enhanced formation of χ-Fe_5C_2 species after the modification by an alkali metal ion except for Li^+ contributes to promoting the selectivities to C_2–C_4 olefins and C_{5+} hydrocarbons (mainly olefins) during the hydrogenation of CO_2. The decreased hydrogenation ability in the presence of an alkali metal ion would also contribute to the increased fraction of C_2–C_4 olefins. Furthermore, the presence of electron-donating K^+ modifier on catalyst surfaces may hinder the re-adsorption of olefins, which were also electron donors, and this may also result in higher olefin selectivities. We further performed a relatively longer-term reaction for the K^+-Fe/ZrO_2 catalyst to investigate the stability of this catalyst containing χ-Fe_5C_2. Fig. 9 demonstrates that both the conversion of CO_2 and the selectivity to C_2–C_4 olefins do not undergo significant decreases after a reaction at 623 K for ~60 h.

Concerning the role of the alkali metal ion in the formation of iron carbide species, through in situ EXAFS/XANES studies, Ribeiro et al. recently showed that the alkali metal ions also accelerated the carburization of iron over an Fe/silica catalyst, i.e., the formation of iron carbides (mainly χ-Fe_5C_2), in a CO/He mixture at 563 K [47]. The rate of carburization was found to increase in the order of unpromoted catalyst < Li-promoted catalyst < Na-promoted catalyst < K-promoted catalyst ≈ Rb-promoted catalyst ≈ Cs-promoted catalyst [47]. Many studies suggested that the presence of an alkali metal ion, particularly K^+, could facilitate the dissociation of CO because of the electronic effect [33,37,47–50]. The changed electron density on Fe species in the presence of K^+ may weaken the C-O bond in CO molecules chemisorbed on Fe surfaces and strengthen the Fe—C bond, accelerating the generation of iron carbide species. Such an electronic effect may also weaken the Fe-H bond, reducing the hydrogenation ability of Fe catalysts [48–50].

To understand the reasons for the differences in catalytic behaviors of K^+-modified Fe catalysts loaded on different supports, we have performed XRD measurements for three typical catalysts, i.e., the K^+-Fe/SiO_2, K^+-Fe/CNT, and K^+-Fe/ZrO_2 catalysts, after reactions. The results displayed in Fig. 10 show that, besides the diffraction peaks ascribed to the support, the peaks attributed to χ-Fe_5C_2 and Fe_3O_4 were observed for the K^+-Fe/ZrO_2 and K^+-Fe/CNT catalysts. On the other hand, only diffraction peaks assignable to Fe_3O_4 could be detected for the K^+-Fe/SiO_2 catalyst. We speculate that absence of the χ-Fe_5C_2 species for the K^+-Fe/SiO_2 catalyst may be responsible for its lower catalytic activity and selectivity (Table 2). It was once reported that iron (II), which was generated during the reduction process, may interact strongly with SiO_2, forming iron silicate [51]. Iron silicate was difficult to be further reduced, and this might hinder the formation of χ-Fe_5C_2. On the other hand, such an iron zirconate cannot be formed although there may exist an interaction between Fe and ZrO_2 [51]. The comparison of the K^+-Fe/CNT and K^+-Fe/ZrO_2 catalysts, both of which could generate χ-Fe_5C_2 phase during the reaction, showed that the former catalyst exhibited relatively higher selectivities to CH_4 and C_2–C_4 paraffins. It is known that CNTs are excellent supports for hydrogenation reactions because of their unique properties in H_2 adsorption and spillover [52,53]. Such an excellent hydrogenation

Please cite this article in press as: J. Wang, et al., Synthesis of lower olefins by hydrogenation of carbon dioxide over supported iron catalysts, Catal. Today (2013), http://dx.doi.org/10.1016/j.cattod.2013.03.031

ability of the CNT-based catalyst may lead to the relatively higher selectivities to CH_4 and C_2–C_4 paraffins. Further studies are needed in the future to clarify why the ZrO_2-supported K^+-modified Fe catalyst can afford better catalytic performances for the formation of C_2–C_4 olefins.

4. Conclusions

The Fe/ZrO_2 catalyst modified by a proper alkali metal ion was found to be an efficient catalyst for the hydrogenation of CO_2 to C_2–C_4 olefins. The Fe/ZrO_2 without modification provided CH_4 and C_2–C_4 paraffins as the main products in the hydrogenation of CO_2. The addition of an alkali metal ion except for Li^+ significantly suppressed the formations of CH_4 and C_2–C_4 paraffins, and promoted the formations of C_2–C_4 olefins and C_{5+} hydrocarbons. K^+ and ZrO_2 were demonstrated to be the best modifier and support of iron catalysts for the hydrogenation of CO_2 to C_2–C_4 olefins. The catalytic performance was also dependent on the content of K^+. Over the K^+-Fe/ZrO_2 catalyst with a proper K^+ content (0.5–1 wt%), the yield of C_2–C_4 olefins could reach 13%, with the fraction of C_2–C_4 olefins in the hydrocarbons being ~45%. The modification of the Fe/ZrO_2 catalyst by K^+ accelerated the generation of χ-Fe_5C_2 species under the reaction conditions. The presence of K^+ also enhanced the adsorption of CO_2 and decreased the hydrogenation ability. These were proposed to mainly contribute to the increase in the conversion of CO_2 and the change in the product distributions in the presence of K^+ modification.

Acknowledgement

This work was supported by the National Basic Research Program of China (No. 2013CB933102), the Natural Science Foundation of China (Nos. 21173174, 21161130522, 21033006, and 20923004), and the Program for Changjiang Scholars and Innovative Research Team in Chinese Universities (No. IRT1036).

References

[1] C.S. Song, Catalysis Today 115 (2006) 2–32.
[2] G. Centi, S. Perathoner, Catalysis Today 148 (2009) 191–205.
[3] A.J. Hunt, E.H.K. Sin, R. Marriott, J.H. Clark, ChemSusChem 3 (2010) 306–322.
[4] Q. Wang, J. Luo, Z. Zhong, A. Borgna, Energy and Environmental Science 4 (2011) 42–55.
[5] A. Goeppert, M. Czaun, G.K.S. Prakash, G.A. Olah, Energy and Environmental Science 5 (2012) 7833–7853.
[6] M. Aresta, A. Dibendetto, Dalton Transactions (2007) 2975–2992.
[7] T. Sakakura, J.C. Choi, H. Yasuda, Chemical Reviews 107 (2007) 2365–2387.
[8] J. Ma, N. Sun, X. Zhang, N. Zhao, F. Xiao, W. Wei, Y. Sun, Catalysis Today 148 (2009) 221–231.
[9] M. Cokoja, C. Bruckmeier, B. Rieger, W.A. Herrmann, F.E. Kühn, Angewandte Chemie International Edition 50 (2011) 8510–8537.
[10] W. Wang, S. Wang, X. Ma, J. Gong, Chemical Society Reviews 40 (2011) 3703–3727.
[11] V.P. Indrakanti, J.D. Kubicki, H.H. Schobert, Energy and Environmental Science 2 (2009) 745–758.
[12] S.C. Roy, O.K. Varghese, M. Paulose, C.A. Grimes, ACS Nano 4 (2010) 1259–1278.
[13] W. Fan, Q. Zhang, Y. Wang, Physical Chemistry Chemical Physics 15 (2013) 2632–2649.
[14] F. Ovampo, B. Louis, L. Kiwi-Minsker, A.C. Roger, Applied Catalysis A: General 392 (2011) 36–44.
[15] A.H. Tullo, Chemical and Engineering News 81 (50) (2003) 15–16.
[16] J. He, T. Xu, Z. Wang, Q. Zhang, W. Deng, Y. Wang, Angewandte Chemie International Edition 51 (2012) 2438–2442.
[17] T. Xu, Q. Zhang, H. Song, Y. Wang, Journal of Catalysis 295 (2012) 232–241.
[18] H.M.T. Galvis, J.H. Bitter, C.B. Khare, M. Ruitenbeek, A.I. Dugulan, K.P. de Jong, Science 335 (2012) 835–838.
[19] U. Olsbye, S. Svelle, M. Bjørgen, P. Beato, T.V.W. Janssens, F. Joensen, S. Bordiga, K.P. Lillerud, Angewandte Chemie International Edition 51 (2012) 5810–5831.
[20] P.H. Choi, K.W. Jun, S.J. Lee, M.J. Choi, K.W. Lee, Catalysis Letters 40 (1996) 115–118.
[21] Z.H. Suo, Y. Kou, J.Z. Niu, W.Z. Zhang, H.L. Wang, Applied Catalysis A: General 148 (1997) 301–303.
[22] H. Ando, Q. Xu, M. Fujiwara, Y. Matsumura, M. Tanaka, Y. Souma, Catalysis Today 45 (1998) 229–234.
[23] L. Xu, Q. Wang, D. Liang, X. Wang, L. Lin, W. Cui, Y. Xu, Applied Catalysis A: General 173 (1998) 19–25.
[24] S.S. Nam, H. Kim, G. Kishan, M.J. Choi, K.W. Lee, Applied Catalysis A: General 179 (1999) 155–163.
[25] M.L. Cubeiro, H. Morales, M.R. Goldwasser, M.J. Pérez-Zurita, F. González-Jiménez, G. Urbina de N, Applied Catalysis A: General 189 (1999) 87–97.
[26] T. Riedel, G. Schaub, K.W. Jun, K.W. Lee, Industrial and Engineering Chemistry Research 40 (2001) 1355–1363.
[27] T. Riedel, H. Schulz, G. Schaub, K.W. Jun, J.S. Hwang, K.W. Lee, Topics in Catalysis 26 (2003) 41–54.
[28] T. Herranz, S. Rojas, F.J. Pérez-Alonso, M. Ojeda, P. Terreros, J.L.G. Fierro, Applied Catalysis A: General 311 (2006) 66–75.
[29] P.S.S. Prasad, J.W. Bae, K.W. Jun, K.W. Lee, Catalysis Surveys from Asia 12 (2008) 170–183.
[30] R.W. Dorner, D.R. Hardy, F.W. Williams, B.H. Davis, H.D. Willauer, Energy Fuel 23 (2009) 4190–4195.
[31] R.W. Dorner, D.R. Hardy, F.W. Williams, H.D. Willauer, Applied Catalysis A: General 373 (2010) 112–121.
[32] E. de Smit, B.M. Weckhuysen, Chemical Society Reviews 37 (2008) 2758–2781.
[33] Q. Zhang, J. Kang, Y. Wang, ChemCatChem 2 (2010) 1030–1058.
[34] P. Chen, H.B. Zhang, G.D. Lin, Q. Hong, K.R. Tsai, Carbon 35 (1997) 1495–1501.
[35] J. Wambach, A. Baiker, A. Wokaun, Physical Chemistry Chemical Physics 1 (1999) 5071–5080.
[36] P. Wang, J. Kang, Q. Zhang, Y. Wang, Catalysis Letters 114 (2007) 178–184.
[37] W. Ngantsoue-Hoc, Y. Zhang, R.J. O'Brien, M. Luo, B.H. Davis, Applied Catalysis A: General 236 (2002) 77–89.
[38] D. Li, N. Ichikuni, S. Shimazu, T. Uematsu, Applied Catalysis A: General 172 (1998) 351–358.
[39] R.A. Fiato, E. Iglesia, G.W. Rice, S.L. Soled, Studies in Surface Science and Catalysis 107 (1998) 339–344.
[40] M.D. Shroff, D.S. Kalallad, K.E. Coulter, S.D. Köhler, M.S. Harrington, N.B. Jackson, A.G. Sault, A.K. Datye, Journal of Catalysis 156 (1995) 185–207.
[41] W. Chen, Z. Fan, X. Pan, X. Bao, Journal of the American Chemical Society 130 (2008) 9414–9419.
[42] E. de Smit, F. Cinquini, A.M. Beale, O.V. Safonova, W. van Beek, P. Sautet, B.M. Weckhuysen, Journal of the American Chemical Society 132 (2010) 14928–14941.
[43] H.M.T. Galvis, J.H. Bitter, T. Davidian, M. Ruitenbeek, A.I. Dugulan, K.P. de Jong, Journal of the American Chemical Society 134 (2012) 16207–16215.
[44] B. Sun, G. Yu, J. Lin, K. Xu, Y. Pei, S. Yan, M. Qiao, K. Fan, X. Zhang, B. Zong, Catalysis Science & Technology 2 (2012) 1625–1629.
[45] C. Yang, H. Zhao, Y. Hou, D. Ma, Journal of the American Chemical Society 134 (2012) 15814–15821.
[46] Q. Zhang, W. Deng, Y. Wang, Journal of Energy Chemistry 22 (2013) 27–38.
[47] M.C. Ribeiro, G. Jacobs, B.H. Davis, D.C. Cronauer, A.J. Kropf, C.L. Marshall, Journal of Physical Chemistry C 114 (2010) 7895–7903.
[48] Y. Yang, H.W. Xiang, Y.Y. Xu, L. Bai, Y.W. Li, Applied Catalysis A: General 266 (2004) 181–194.
[49] N. Lohitharn, J.G. Goodwin Jr., Journal of Catalysis 260 (2008) 7–16.
[50] R. Luque, A.R. de la Osa, J.M. Campelo, A.A. Romero, J.L. Valverde, P. Sanchez, Energy and Environmental Science 5 (2012) 5186–5202.
[51] F.R. van den Berg, M.W.J. Crajé, P.J. Kooyman, A.M. van der Kraan, J.W. Geus, Applied Catalysis A: General 235 (2002) 217–224.
[52] H. Zhang, X. Dong, G. Lin, X. Liang, H. Li, Chemical Communications 40 (2005) 5094–5096.
[53] J. Kang, S. Zhang, Q. Zhang, Y. Wang, Angewandte Chemie International Edition 48 (2009) 2565–2568.

Please cite this article in press as: J. Wang, et al., Synthesis of lower olefins by hydrogenation of carbon dioxide over supported iron catalysts, Catal. Today (2013), http://dx.doi.org/10.1016/j.cattod.2013.03.031